The potentials of high-resolution photogrammetry for analyzing glacier retreat in the Ötztal Alps, Austria

Joschka Geissler[1,4], Christoph Mayer[2], Juilson Jubanski[1], Ulrich Münzer[3] & Florian Siegert[1]

[1]3D Reality Maps GmbH, Dingolfinger Str. 9, Munich, 81673, Germany
5 [2]Bavarian Academy of Science, Geodesy and Glaciology, Alfons-Goppel Str. 11, Munich, 80539, Germany
[3]Ludwig-Maximilians-University, Department of Earth and Environmental Sciences, Section Geology (remote sensing), Luisenstr. 37, 80333 Munich, Germany
[4]Faculty of Environment and Natural Sciences, Albert-Ludwigs University Freiburg, Friedrichstr.39, 79098 Freiburg, Germany

10 *Correspondence to*: Florian Siegert (Siegert@realitymaps.de)

Abstract. Glaciers all over the world experience an increasing mass loss during recent decades due to change in the global climate. This leads to considerable environmental consequences in the densely populated Alps and many other mountain ranges in the world. We used high-resolution aerial photogrammetry within the AlpSenseBench project to investigate glacier retreat in great spatial and temporal detail in the Ötztaler Alps, a significant glacier

15 area in Austria. Long-term in situ glaciological observations are available for this region, and a multitemporal time series of digital aerial images with a spatial resolution of 20 cm acquired over a period of 10 years exists. Glacier retreat of all 25 glaciers in the region, including the Vernagtferner, was analyzed by investigating glacier extent and surface elevation changes, derived from the aerial images by digital surface model (DSM) generation. Due to different acquisition dates of the large scale photogrammetric surveys and the glaciological data, a correction was

20 established using a dedicated unmanned aerial vehicle (UAV) survey across the major part of the Vernagtferner. This allowed us to compare the mass balances from geodetic and glaciological techniques, which reveals the potentials of the combination of these two techniques for gaining a better insight into glacier changes and its spatial distribution. The results show a clear increase of glacier mass loss for all glaciers in the region, including the Vernagtferner over the last decade. Additionally, the influence of debris-cover on mass balance, as well as the

25 magnitude of dynamic processes, could be quantified. The comparison of geodetic elevation differences and the interpolated glaciological data reveals that there exists a high potential in detecting local peculiarities of mass balance distribution and for correcting small scale deviations, not revealed in the interpolated glaciological information. The availability of high resolution multi-temporal digital aerial imagery for most of the glaciers in the Alps will provide a more comprehensive and detailed analysis of climate change-induced glacier retreat.

30

1   Introduction

The impacts of climate change are widespread and clearly visible in the Alps (Rogora et al., 2018) but particularly evident in the dwindling glacier resources (Sommer et al., 2020; Zekollari et al., 2019). Over the past 100 years, the temperature in the Alps has increased almost twice as fast compared to the global average, resulting in nearly

35   2 °C higher mean air temperatures (Auer et al., 2007; Marty and Meister, 2012). By the end of this century, mean air temperatures are expected to further rise by several degrees Celsius (Gobiet et al., 2014; Hanzer et al., 2018). Due to this ongoing climate evolution, alpine glaciers may lose half of their volume by 2050 compared to 2017 (Zekollari et al., 2019). The response of glaciers to climatic variations is directly related to the mass and energy balance at the glacier surface. Internal deformation and basal sliding redistribute ice from regions with mass gain

40   (accumulation) to regions with mass loss (ablation), compensating the local imbalance with some lag in the response. Changes in glacier geometry, however, can be directly related to the mass balance if integrated across the entire glacier. Thus, the geodetic, glacier mean mass change (considering a volume to mass conversion) can be directly compared to glaciological mass balance measurements, based on local ablation and accumulation data.

We focused on a study site within the Ötztaler Alps, Austria, including the Vernagtferner, one of the reference

45   glaciers in the World Glacier Monitoring Service (WGMS) system. Mass-balances have been determined here using the glaciological method since 1965, while a series of historical maps back to 1889 demonstrates the long-term glacier evolution over more than a century.

Digital photogrammetry has been established as the standard method for cadastral surveys during the first decade of the new millennium. It is also used by BEV (Bundesamt für Eich- und Vermessungswesen, Austria) for their

50   periodical digital elevation updates. Consequently, an immense imagery database has been generated, which allows three-dimensional reconstruction and mapping of vast areas in the Alps with a resolution in the order of decimeters. Thereby horizontal and vertical changes can be detected and analyzed on a large scale and with unmatched precision. Combining high-resolution photogrammetry with the extensive knowledge data base for the Vernagtferner acquired over more than a century, this study presents a unique combination of methods that allows

55   the extraction of relevant glaciological information (glacier retreat and mass balances) with greater accuracy from aerial imagery. Data suitable for photogrammetric processing were available in three epochs over a period of 9 years (2009, 2015, 2018), and appropriate in situ observations were used to evaluate and improve the remote sensing information.

The workflow was applied for all 25 glaciers within the study area, including the Vernagtferner. Past studies

60   already demonstrated the potential of spatiotemporal change analysis of alpine glaciers using photogrammetric data (Fugazza et al., 2018; Legat et al., 2016; Rossini et al., 2018). Though, geodetic mass balances from photogrammetry are often restricted by acquisition times and, therefore, not comparable with fixed date glaciological measurements (Fischer, 2011). In this study, a correction due to differences in acquisition dates between photogrammetric and glaciological data is achieved by employing an additional unmanned aerial vehicle

65   (UAV) survey. This calibration allows a parametrization between photogrammetry and glaciology, revealing further potentials for these two techniques for accessing a more accurate insight into glacial retreat.

2   Study Area

The Ötztaler Alpen are located in the central-eastern Alps and represent one of the most extensive glaciated regions of Austria. The study area ranges from an altitude of 1.700 m to 3.768 meter above sea level (m.a.s.l.) and covers

70   an area of more than 250 km² (Fig. 1). It combines the upper regions of the drainage basins of Rofental, Pitztal, and Kaunertal. The location in the inner part of the Alps leads to relatively low precipitation amounts (Fliri, 1975), which for example, reach mean values of 660 mm yr^{-1} at the valley station Vent in 1969-2006 (Abermann et al., 2009). For some of the 25 glaciers within the study site exist periods of mass balance measurements. One of the longest series of measurements is at the Vernagtferner, where regular monitoring by the Bavarian Academy of

75   Sciences and Humanities (BAdW) began in 1965. This glacier is characterized by several sub-basins, which were connected to a single glacier tongue in former times. Today the glacier covers an area of almost 7 km² within an altitude range between 2860 m and 3570 m. The mass balance is determined by the glaciological method, using measurements at ablation stakes, manual and geophysical depth soundings, and retrieving information from snow and firn pits. The annual and winter mass balances are determined independently of each other by measurements

80   on the fixed dates of May 1st and September 30th, the dates of the glaciological balance year (Cogley, 2010; Cogley et al., 2011). Besides, there is a long history of geodetic mapping at the Vernagtferner dating back to 1889 (Mayer et al., 2013a).
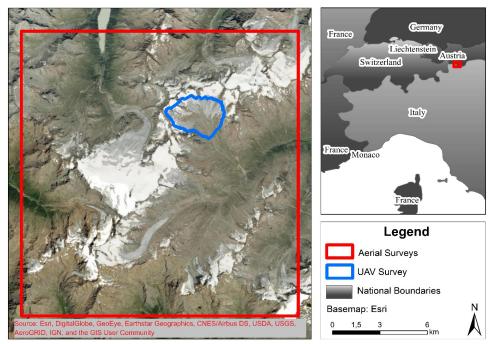

Figure 1: Study site in the Ötztaler Alps; Red: area covered by aerial surveys; Blue: area of the Vernagtferner covered
85   **by the UAV Survey (Esri et al., 2020)**

3

The Cryosphere
Discussions
Open Access
EGU

3 Data Acquisition

3.1 Photogrammetric data acquisition

After the introduction of the first large format digital aerial photogrammetric camera in 2000, this type of sensor
quickly became the standard equipment for aerial surveys. The replacement of analog to digital equipment not
90 only dramatically reduced the surveying costs, but also enabled the development of advanced three-dimensional
high-resolution reconstruction algorithms based on photogrammetry (Heipke, 2017; Hirschmüller, 2019). This
kind of reconstruction works best with horizontal overlaps of more than 80%. Digital sensors allow surveys with
this overlap because the high costs for photographic negatives no longer exist. Since the late 2000s, European state
surveying agencies have been carrying out cadastral surveys every two to four years with digital sensors and
95 horizontal overlap of 80%, thus creating an immense multitemporal database of aerial imagery to be explored both
commercially and scientifically.

In Austria, cadastral aerial surveys are conducted by the BEV with a nominal resolution of 20 cm. We use a BEV
survey from 2015 as a basis for our investigations. Besides, surveys performed by 3D RealityMaps in 2009 and
2018 with the same or higher ground resolution are investigated. Table 1 shows the most relevant information on
100 the conducted air surveys.

In addition to the airplane based surveys, a smaller test site was covered by UAV flights to retrieve high-resolution
data at another acquisition date closer to the maximum of ablation in 2018 (Table 1). The processed area covers 6
km² containing most the glacier area of the Vernagtferner, including all glacier tongues. The glacier was almost
snow-free at the time of the acquisition, which provides optimal processing conditions.

105

Table 1: Overview of the aerial data acquisitions

Date	Platform	Area	Overlap	Resolution	Images	Image type	Camera
09.09.2009	Airplane	257 km²	80:40	20 cm	381	TIF RGB 8bit	UltraCam XP
03.08.2015	Airplane	330 km²	80:50	20 cm	572	TIF RGBI 16bit	UltraCam XP
21.09.2018	Airplane	260 km²	80:60	20 cm	428	TIF RGBI 16bit	UltraCam Eagle Mark 2
21.08.2018	UAV	6 km²	80:80	5 cm	1992	JPEG RGB 8bit	UMC-R10C

3.2 Glaciological data acquisition

Glaciological mass balance data are acquired at the Vernagtferner since 1965. Information is gathered as stake
110 readings from ablation stakes for estimating the ice melt across the glacier. At the same time, snow depth and last
season firn deposits are determined from mechanical depth soundings with metal probes, which are then combined
with density information from snow and firn pits to calculate the ice per water equivalent of the remaining snow
and firn cover. While stake readings only require two length measurements per stake with an uncertainty of
typically about 1 cm, more significant errors are included in the direct accumulation measurements due to
115 uncertainties in the sample volume (about 5%) and the determination of density by using spring scales (about 4%).

4

Therefore water equivalent accuracy is about 6% (Zemp et al., 2013). The typical number of stakes used for the annual mass balance measurements at the Vernagtferner is about 35, while some 4-5 accumulation measurements are collected at the end of the glaciological year, September 30th. The equilibrium line, which represents a mass balance of zero, is derived by comparing oblique terrestrial photographs of the transient snow line and firn extent

120   with optical remote sensing information close to the date of the field measurements. The derived equilibrium line has a horizontal location accuracy of about 10 m. Glacier boundaries for delineating the spatial mass balance distribution are derived from aerial surveys repeated roughly each decade, which are updated in the ablation region by annual GNSS (Global Navigation System Services) measurements of the glacier tongue geometry. The spatial error of these measurements is usually better than 1 m. The information from the stake readings, the depth

125   soundings, the snow pits, and the location of the equilibrium line are combined to interpolate the spatial distribution of the glacier mass balance into a raster file. Due to the sparse information in the accumulation region, it is necessary to manually correct the interpolation results in this region by the knowledge of the long term accumulation patterns, which are rather persistent. Errors introduced by uncertainties in the accumulation region, however, are rather small, especially during the recent decade where the accumulation area ratio is usually well

130   below 30%. While ablation varies between 0 and up to 4500 mm in the ablation area, accumulation only varies between 0 and about 300-400 mm in the accumulation area. Within this study we assumed the error of the interpolated raster to be 100 mm, which is in accordance to Zemp et al., 2013. It must be noted, that this relatively large error within the accumulation area will only affect the final mass balance by less than 2%.

4   Methods

135   ### 4.1   Photogrammetric workflow

In order to determine geodetic glacier mass balances from aerial and UAV images, we use a workflow consisting of two main modules: the data processing and the vertical change analysis (Fig. 3). The main goal of the data processing module is the reconstruction from raw imagery data into 3D point clouds. Digital surface models (DSM) and true orthophoto mosaics (TOM) are then derived from these point clouds. Finally, DSM differences

140   are computed. Within the vertical change analysis module, geodetic glacier mass balances are computed from the DSM differences.
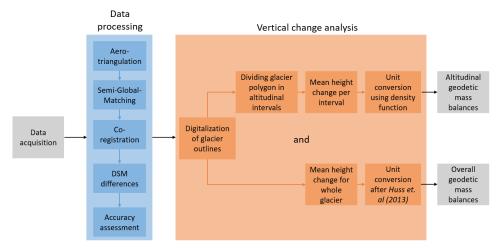
Figure 2: Full photogrammetric workflow; Blue: From raw images to DSM differences; Orange: From DSM differences to overall and altitudinal mass balances

4.1.1 Data processing

The first step in data processing is the aerotriangulation, which consists of the orientation of the aerial imagery to the real terrain. Modern photogrammetric survey systems deliver highly accurate position (GNSS) and orientation (IMU, inertial measurement unit) information for each image, which are also included in the aerotriangulation for the georeferencing. Finally, at least 20 tie points were manually identified for each image block to enhance the orientation accuracy. For the large format imagery, the aerotriangulation was performed using the state of art software *Match-AT* by Trimble. For the UAV imagery, the software *Metashape Professional* from Agisoft was used.

The second stage of data processing is the generation of point clouds through three-dimensional reconstruction. For this purpose, the state of the art Semi-global-matching algorithm (Heipke, 2017; Hirschmüller, 2019) was used. This algorithm is implemented within the software *SURE* (nFrames), which generates DSM and TOM from the point clouds. Positioning accuracies of TOM and DSM were computed based on ground control points from the BEV. The horizontal shift lies between 10 and 20 cm depending on the acquisition year and thus within the ground resolution of the images.

In order to calculate the DSM differences, existing systematic height shifts were corrected by using stable areas (mostly large rock formations) outside the glaciers. The 2015 DSM was chosen as the reference because it was derived from the official Austrian cadastral survey and is referenced to the Austrian national survey system. The mean shift in elevation compared to the reference DSM was computed based on 50 identified stable points, e.g., on solid rocks, for each DSM and 21 stable points for the UAV-survey. Based on this mean vertical shift over stable ground, all DSMs except for the reference DSM were adjusted in height relative to the reference DSM of 2015. Subsequently, the DSM differences 9/2018–8/2015, 8/2015–9/2009, 9/2018–9/2009, and 9/2018–8/2018 were computed and named after their acquisition dates.
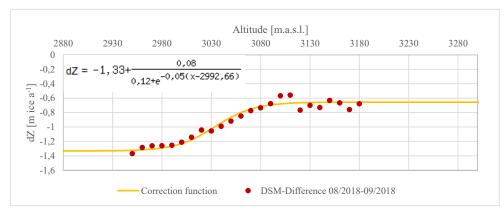
6

4.1.2   Vertical change analysis

170   For the vertical change analysis (Fig. 2, orange part), glacier outlines were digitized visually using the TOMs at a scale of 1:2.000. The geodetic glacier mass balance (B) for a single glacier is determined by integrating the DSM difference over the glacier outline at the beginning of the respective period. The result is divided by the mean glacier area of the period. More details can be found, for instance, in Fischer et al., 2015b. For the conversion in mm water-equivalent (w.e), the density assumption proposed by Huss, 2013, 850 kg m^{-3} ± 60 kg m^{-3}, was used. To

175   determine altitudinal dependencies of the glacier mass balances, the glacier polygons were divided into 10 m altitudinal intervals additionally. For each altitudinal interval, the mean absolute height change in meters was determined as well. For the conversion in mm w.e., an altitude-related density functions was used. It represents the gradual change from ice density (900 kg m^{-3}) in the ablation region to firn density (550 kg m^{-3} (Cogley et al., 2011)) in the accumulation region, by using a linear transition zone of ±50 m across the equilibrium line altitude

180   (ELA).

4.2   Comparison with glaciological data

To be able to compare the mass balances determined glaciologically and photogrammetrically, they must have the same period. For this purpose, the annually available glaciological mass balances were accumulated to the periods 09/2009-09/2015, 09/2015-09/2018, and 09/2009-09/2018. The acquisition dates of the photogrammetric data

185   differ from the glaciological measurements (Table 2). To account for the temporal differences, which are limited to the period of maximum ablation in August and September, the photogrammetric DSM difference 08/2018–09/2018 was used. From this, a correction function (sigmoid, see Fig. 3) was derived. For the regression, only those altitude levels were considered, which were at least 40 % covered by the UAV survey. The SD of the regression is 0.07 m ice a^{-1} (Fig. 3). Above 3180 m.a.s.l., thus, for the accumulation areas, the correction function

190   is not based on any data and is therefore error-prone. Additionally, for the correction of the time periods, it had to be assumed that the ablation process was constant during the period between August 21st and September 21st, 2018, and that the magnitude was comparable to the years of 2009 and 2015.

195   **Figure 3: DSM difference in 10 m altitude bands for the period 08/2018–09/2018 (red dots); Correction function (yellow) for acquisition date correction, representing height changes related to the altitude within one month in August and September 2018; SD of the regression is 0.07 m ice a^{-1}.**

The Cryosphere
Discussions
EGU
Open Access

Subsequently, the DSM differences were adjusted according to the number of days the investigation periods differ

200   using a correction factor, and the correction function (Table 2). The correction factor converts the number of deviating days into months, thus represents the factor of which the monthly ablation (correction function) is added to the respective DSM difference.

Table 2: Correction of photogrammetric DSM differences due to differences in acquisition dates; The Correction factor
205   **is computed by dividing the number of days that deviate through 30 days per month.**

DSM difference	Acquisition date photogrammetric data		Acquisition date glaciological data	Deviation Number of days [days]	Correction Factor [months]
09/2009-09/2018	09.09.2009	21.09.2018	30st of September each year	-12	- 0,4
09/2009–08/2015	09.09.2009	03.08.2015	30st of September each year	37	+1,2
08/2015–9/2018	03.08.2015	21.09.2018	30st of September each year	-49	-1,6

Subsequently, for the density conversion of the adjusted DSM differences 2009–2018, 2009–2015, and 2015–2018, the altitude related density assumption (4.1.2) was used. Finally, the adjusted DSM differences were subtracted from the corresponding accumulated glaciologically derived rasters (sect. 3.2). The resulting Variation

210   Rasters show the spatial deviations between the two methods. Using the Variation Raster, local methodical deviations (e.g. debris cover or crevassed areas) were quantified. Therefore, the respective areas were manually digitized, and the mean value of the Variation Raster was calculated. This value can be related to the total mass balance to estimate the magnitude of methodological errors.

4.3   Vertical accuracy assessment

215   To assess the error distribution within the study area after the coregistration, 1.5 km² of ice-free, stable terrain were analyzed representing a wide range of slope, aspect and altitude. Therefrom, the mean shift as well as the standard deviation within those areas was calculated and their relation to topography was investigated, following Nuth and Kääb, 2011.

To estimate the error when averaging over extended areas, we followed Rolstad et al., 2009, by assessing the
220   spatial covariance of the elevation differences with the use of semivariograms. For the application of the method, we assumed that elevation difference are constant in space, no large-scale trends and that there is no significant variation of the variance in space.

Basic error propagation was implemented (Nuth and Kääb, 2011) in order to determine the compound error of DSM differences, density conversion (7 %, sect. 4.1.2, Huss, 2013), the correction function of the acquisition
225   dates (SD = 0.07 m ice a^{-1}, sect. 4.2) as well as the error associated to the glaciological interpolation raster (sect. 3.2) for all presented results. The error within this study is indicated by the 95% confidence interval.
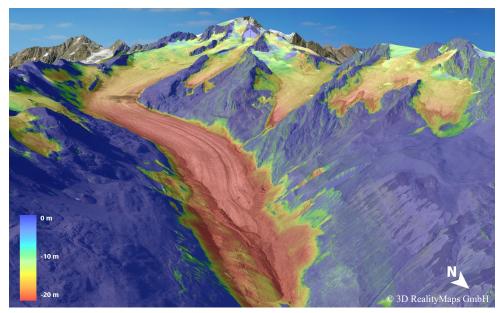
5   Results

5.1   Vertical Change Analysis

5.1.1   Visual assessment

230   Using the photogrammetrically derived glacier outlines, TOMs, as well as the DSM differences, the first results are obtained by a visual interpretation for the entire study area. In general, glaciers were losing mass during the recent decade and thus are declining in terms of their size and ice thickness. For instance, the glacier tongue of the Hintereisferner has lost more than 20 m in height during the nine years from 09/2009 to 09/2018 (Fig. 4) With increasing altitude, the loss of height on the glacier approaches zero. Analyzing the TOM of the three surveys,

235   reveals that the eastern part of the Hochjochferner lost a considerable area along its lower glacier margin. Especially its main tongue shortened, not considering remaining dead ice bodies, by 826 m between 2009 and 2018 (Fig. 5). A further visualisation of this evolution can be assessed at https://og.realitymaps.de/AlpSense/.

240   **Figure 4: Visual representation of the height differences between the DSMs of 09/2009 and 09/2018 for Hintereisferner. Surface height differences are color-coded. Ice loss is especially high at altitudes below 2.500 m.**
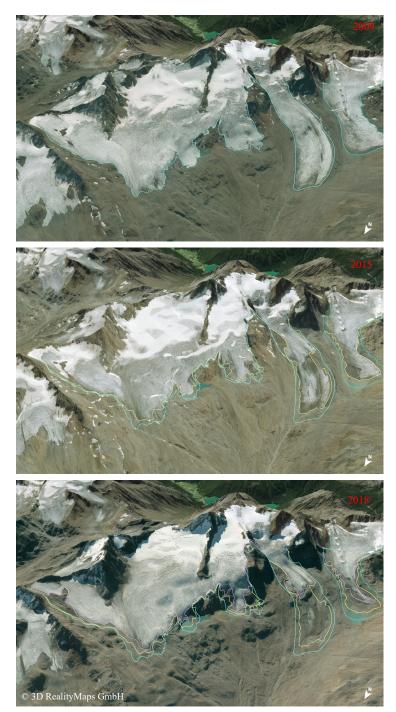
9

Figure 5: Visual assessment of the length change for the Hochjochferner; Lines indicate glacier extent for the respective years. The glacier tongue in the center-right lost 826 m in 9 years.
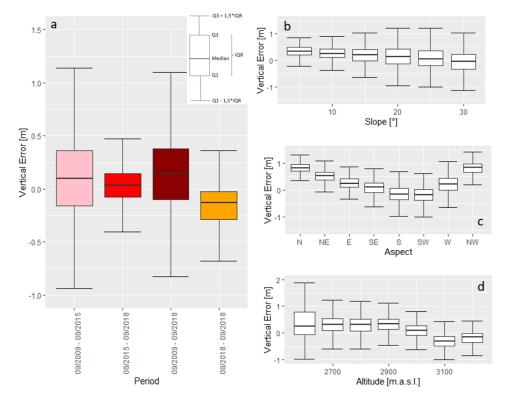
5.1.2 Vertical accuracy assessment

The accuracy assessment conducted (sect. 4.3) allows an estimation of potential error related to the DSM differences and derived products. In general, the mean vertical error of the DSM differences ranges from -0.16 m

250 to 0.1 m with SD not exceeding 0.42 m (Fig. 6a). As expected, SD increases with the slope (Fig. 6b). A clear increase of the SD can also be found in lower altitudes (< 2600 m.a.s.l., (Fig. 6d), most likely due to the increasing influence of vegetation. A relation between aspect and the vertical error was found (Fig. 6c), that can be attributed to the horizontal shift of the DSMs (see sect. 4.1.1) (Nuth and Kääb, 2011).

Based on the error assessment, the confidence interval for all results within this paper was determined. Therefore,

255 semivariograms were computed for the 1.5 km² bedrock areas for all observation periods, from which the range-value (100 m) was conducted and converted to the correlated area value (31416 m²). For more detailed information of this method see Rolstad et al., 2009.

260

Figure 6: Error assessment of the DSM differences in general (a) and in relation to topography (right); Boxplots in the right column have been plotted using the DSM difference 09/2009- 08/2015

5.1.3 Mass balances

Mass balance analysis was focussed on the Vernagtferner because of data availability. It must be considered that

265 the height changes per altitude are not equal to the glaciological vertical balance profile of a glacier, because there are still contributions of firn processes and ice dynamics included in the signal. However, the mean annual height

changes per altitude show a characteristic shape with the highest losses at the glacier tongues and a large difference between the investigation periods of 09/2009-08/2015 and 08/2015-09/2018 (Fig. 7, bottom). However, it needs to be considered that the investigated periods do not cover full mass balance years, which influences the annual

270 mean values considerably. Therefore height changes for the Vernagtferner were corrected (as described in sect. 4.2) to scale the results to full mass balance years (Fig. 7, top left). After the correction, there remains a difference in height change between the two periods, albeit considerably smaller. The later period between 2015-2018 generally shows more negative values than during the period 2009-2015, which now also affects the highest elevations of the glacier.

275 Based on the area distribution by altitude, the volume change per 10 m height interval can be calculated from the annual height changes After correcting for the acquisition dates, the elevation of maximum annual volume loss and its magnitude clearly increased between the investigation periods. Specifically, based on the regression curve (gaussian fit) for the corrected values of the Vernagtferner, 0.21 ± 0.01 Million m³ a^{-1} was lost at an altitude of 3009-3019 m.a.s.l. between 2009 and 2015, while the amount and altitude of the maximum volume loss increased

280 to 0.29 ± 0.02 Million m³ a^{-1} at 3089-3099 m.a.s.l. for 2015-2018 (Fig. 7).
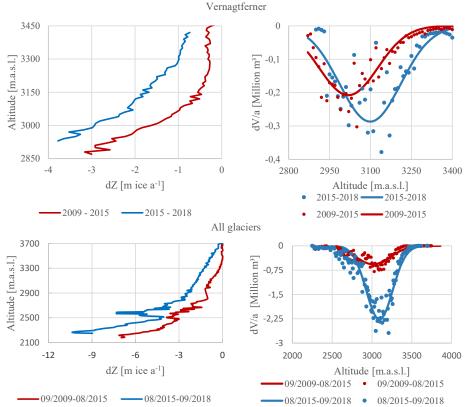

Figure 7: Left: Annual height changes per altitude for the Vernagtferner (top) and all glaciers (bottom); right: annual
285 **volume changes for the Vernagtferner (top) and all glaciers (bottom); Values after correction of acquisition dates to glaciological balance years.**

5.2 Comparison with glaciological measurements

The photogrammetric, as well as the glaciological mass balances of the Vernagtferner, were further compared to detect discrepancies in spatial distribution or magnitude between both methods presented. Therefore, the DSM differences, as well as the overall geodetic mass balances, were compared to the equivalent accumulated glaciologically derived mass balances. At the same time, the correction of the acquisition dates is evaluated. As already noted, the overall mass balance for the Vernagtferner is more negative in the period 2015-2018 than in the period 2009-2015. This can be seen in both, the glaciological and the geodetic mass balances (Fig. 8). The uncorrected photogrammetric mass balance (blue) does not equal the corresponding glaciological mass balance (orange). After the correction of acquisition dates (red), the photogrammetrically derived geodetic mass balance has approached to the glaciological data. However, the corrected data is still lower for the period 2015 – 2018 and higher for the period 2009 – 2015. This suggests, that the correction for the acquisition dates underestimated the melting processes. For the period 2009 – 2018, where the correction function has lowest impact due to i) a longer time period and ii) lowest number of deviating days (Table 2), the corrected photogrammetric data lies within the error bars of the glaciologic data.
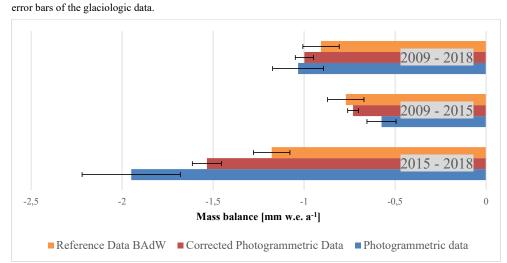

Figure 8: Comparison between photogrammetric mass balances (blue) and glaciological mass balances (orange) for the investigation periods. Red bars visualize corrected photogrammetric data.

The spatial differences between both methods were further investigated using the Variation Raster described in sect. 4.2. The Variation Raster represents spatially distributed deviations of the interpolated rasters based on the glaciological field measurements from the corrected DSM differences based on photogrammetric data (sect. 4.1.1, Fig. 10).

High spatial variations occur in debris-covered areas (red in Fig. 10), where photogrammetrically derived mass balances are higher than glaciological mass balances. Since no ablation stakes are located in supra-glacial debris at the Vernagtferner, the glaciological mass balances for these areas are interpolated from surrounding information on clean ice. Debris cover above a certain thickness protects the glacier against incoming heat fluxes (Östrem, 1959) and therefore reduces the ablation. For the entire Vernagtferner, the neglect of debris-covered areas within

13

glaciological interpolation lead to an underestimation of the glaciological mass balance by about 0.1 m ± 0.08 w.e.

315   a⁻¹ (0.8 ± 0.6 %).

Further analysis of the Variation Raster (Fig. 10) emphasizes that photogrammetric and glaciologically derived mass balances do not only differ spatially due to debris cover or other external effects. It is also evident that the deviations depend on the altitude. Thus, in the lower reaches of the glacier, photogrammetric mass balances are higher than the glaciological mass balances. For higher altitudes, photogrammetric mass balances are lower than

320   the glaciologically derived ones. This pattern is usually attributed to the ice dynamic component of elevation change contained in the geodetic differences (submergence and emergence of ice and firn). Additionally, Fig. 9 clearly shows that comparing the different observation periods, the bias between both methods becomes larger within the accumulation areas.
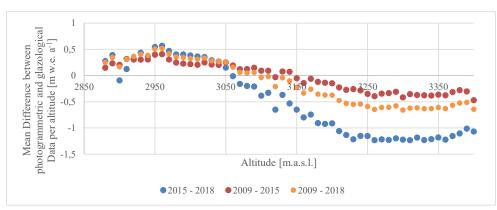
325

Figure 9: Comparison of photogrammetric DSM differences and accumulated glaciologically derived mass balances depending on altitude [m w.e. a⁻¹] after the correction of acquisition dates

330   Assuming all deviations between photogrammetrically and glaciologically derived DSM differences (Fig. 9) are caused by dynamic processes, the magnitude of emergence and submergence is computed. Between 2009 and 2018, the mean emergence (between 2900 m.a.s.l. and 3050 m.a.s.l.) is 0.34 m w.e. a⁻¹ ± 0.25 m w.e. a⁻¹, with a maximum at 0.52 m w.e. a⁻¹. Submergence occurs at altitudes higher than 3150 m.a.s.l. and results to a mean of - 0.48 m w.e. a⁻¹ ± 0.25 m w.e. a⁻¹, with a maximum of -0.65 m w.e. a⁻¹ ± 0.25 m w.e. a⁻¹ (Fig. 10). For a glacier in

335   balance, the change between submergence and emergence regions occurs close to the equilibrium line. However, the mean ELA of the Vernagtferner is about 3250 m for the period 2009-2018 and thus roughly 150 m higher than the switch between apparent emergence and submergence.

The comparison of the five different accumulation basins of the Vernagtferner shows that the mean differences are greater for higher basins with the largest offsets for the remaining true accumulation regions Hochvernagt,

340   Brochkogel and Taschachhochjoch.

14

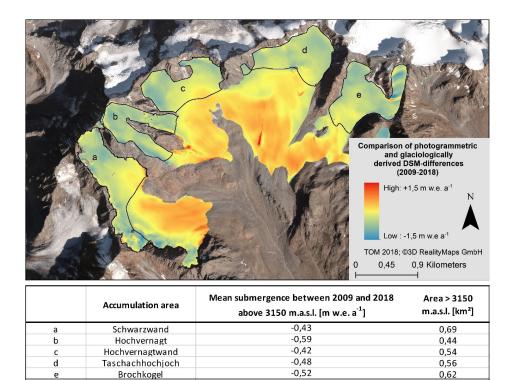|	Accumulation area	Mean submergence between 2009 and 2018 above 3150 m.a.s.l. [m w.e. a^{-1}]	Area > 3150 m.a.s.l. [km²]
a	Schwarzwand	-0,43	0,69
b	Hochvernagt	-0,59	0,44
c	Hochvernagtwand	-0,42	0,54
d	Taschachhochjoch	-0,48	0,56
e	Brochkogel	-0,52	0,62
	Vernagtferner	**-0,48**	**2,85**

Figure 10: Top: Variation Raster 2015–2018: Comparison of the corrected photogrammetric DSM differences and glaciologically derived data; Blue areas symbolize glaciologically derived DSM differences being higher than the photogrammetric DSM differences. In red areas, glaciologically obtained DSM differences are lower than the photogrammetric DSM differences. For regions that appear yellow, both methods present similar height changes.; Black outlines represent the different accumulation areas of the Vernagtferner; The mean submergence is given for each accumulation area in m w.e. a^{-1}, having an associated error of ± 0.25 m w.e.

5.3 Other glaciers within the study site

The major advantage of the photogrammetric mass balance assessment is that large areas can be investigated in detail. Therefore, we investigated the geodetic mass balance of all glaciers in the study area. The mean height difference over the glacier surface was determined and converted into m w.e. as described above. The mean mass balance of all glaciers was -0.38 ± 0.05 m w.e. a^{-1} for 09/2009–08/2015, while it quadruples to -1.61 ± 0.22 m w.e. a^{-1} between 08/2015 and 09/2018. It must be noted that there was no correction applied for the acquisition times. Accordingly, the mass balances do not refer to identical annual periods. However, if a time correction is assumed to have a similar influence on the annual mass balances of other glaciers as it had for the Vernagtferner (-27% for 09/2009-08/2015 and +21% for 08/2015–09/2018, Fig. 8), the mean mass balances of all glaciers can be estimated. Accordingly, the mean annual glacier mass balance within the study area would be -0.48 ± 0.06 m w.e. a^{-1} for the period 2009-2015 and -1.26 ± 0.06 m w.e. a^{-1} for the period 2015-2018. The comparative values for the Vernagtferner exceed those values by 51% and 21%, respectively (Fig. 8). Figure 11 compares the altitude-related height losses of the Vernagtferner to the mean of all glaciers of the study area and the Hintereis- and Hochjochferner (Fig. 4 and Fig. 5).
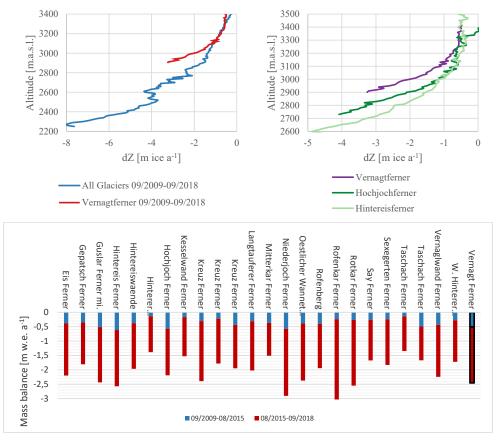
15

Figure 11: Annual height changes per altitude between 09/2009 and 09/2018 for the Vernagtferner compared to (i) all glaciers within the study area (top left) and (ii) to the Hochjochferner and Hintereisferner (top right); Comparison of all glacier mass balances within the study area for the two investigation periods

6   Discussion

In this study, we investigated multitemporal changes in surface heights of selected glaciers in the Ötztaler Alpen. We found that, for the Vernagtferner, glacier mass loss accelerated within the last decade. At the same time, the absolute surface height changes showed a maximum at low altitudes for all glaciers (Fig. 7). As it was shown for the Vernagtferner, peak volume loss occurs at higher altitudes, compared to the altitude where maximum height losses occur, since the volume is directly linked to the area-height-distribution of a glacier. These findings correspond to general observations (i) for the Vernagtferner (BADW, 2019; Escher-Vetter, 2015) and (ii) for most of the glaciers in the Alps (Fischer et al., 2015b; Fischer et al., 2015a; Huss, 2012). This study showed the great potential of using photogrammetry for glacier studies. Thus, height changes can easily be investigated for large areas with high spatial resolution and accuracy. As a result, for instance, we were able to estimate the decrease in length of the Hochjochferner (826.4 m ± 0.2 m) between 09/2009 and 09/2018 (Fig. 5) and the maximum height changes at the glacier tongue of Hintereisferner, as shown in Fig. 4 (– 20.4 m ± 0.4 m) with an accuracy of 0.2 m and 0.4 m respectively. A similar analysis and visualization could easily be applied to all the other glaciers within

16

380   the study site. Furthermore, dead ice bodies can be mapped very well using the high-resolution photogrammetric data. For instance, on the north-facing side of the valley, below the glacier tongue of Hintereisferner, a large dead ice body is visible and ice loss could be determined for this feature, which is not included in the glaciological mass balance measurements (Fig. 4). Another result derived from the DSM differences is the vertical surface height changes as a function of elevation (Fig. 7). Even though they cannot be compared to glaciologically derived vertical

385   balance profiles directly, they illustrate (i) the relation of height losses to altitude (Kaser et al., 2003; Pellikka and Rees, 2010) and (ii) a shift between the two observation periods.

    Moreover, the comparison of the uncorrected photogrammetric total mass balances reveals the great potential of photogrammetry for glacier analysis. A large number of glaciers may be analyzed with a high spatial resolution and for the exact same time. For the Ötztaler Alps, based only on the photogrammetric DSM differences, we found

390   that the elevation change (i) is on average lower compared to the Vernagtferner, (ii) is correlated to the altitude of the glacier tongue and (iii) increased between 09/2009–08/2015 and 08/2015–09/2018 (Fig. 11).

    The error assessment conducted reveals the high precision of the photogrammetric data with SD not exceeding 0.42 m for all DSM differences (Fig. 6). Moreover, the variation of the vertical error is normally distributed. A relation was found for the vertical error regarding the aspect, which is presumably based on the vertical shift of

395   the DSM (see sect.4.1.1). The error caused by the relation to the aspect can cause a larger error than the value we suggest, especially for glaciers with homogeneous orientations. Nevertheless, the 95% confidence interval used in this study covers most of these variations. (Fig. 6). Future studies, that want to deduct this error, may follow the methodology suggested by Nuth and Kääb, 2011.

    Semivariograms determined in order to assess the error for averaged values prove that this assumption was

400   possible, since semivariance approximates a clear sill (further information on the method can be found in Rolstad et al., 2009).

    We used the density assumption of Huss, 2013 to convert height changes to water equivalent. It must be noted that the DSM difference 08/2015 – 09/2018 does not fulfill the prerequisite for this assumption, being a period shorter than three years. However, since the accumulation area ratio at the Vernagtferner is relatively small, the density

405   of the lost volume will be close to the density of ice (900 kg/m³), this seems to be a good assumption.

    To adjust photogrammetric mass balances to the acquisition time of the glaciologic measurements (September 30th), a correction was applied. An additional UAV survey was conducted, which made it possible to assess vertical height changes during the last month of the ablation period in 2018 (Fig. 3). Therefrom, a regression function (sigmoid) was determined to correct the offsets of the acquisition dates in 2009, 2015, and 2018. The

410   correction includes an uncertainty for the accumulation areas since the UAV survey did not cover the entire glacier area. Additionally, the intra-annual variation of melting and snowfall introduces another unknown, but important, source of error. More precisely, the transfer of the correction function from September 2018 to another year (here September 2009 and 2015) is strongly dependent on the meteorological conditions of the specific period. For instance, a snowfall event shortly before the survey would introduce an unknown error. The retrospective

415   correction of the time periods therefore is not more than an approximation to the glaciological values. This uncertainty must be taken into account, in particular for the shorter observation periods 2009-2015 and 2015-2018, where the correction has a higher impact (Table 2). This might explain that the deviations to the glaciological data increase for shorter periods (Fig. 8). Thus, we focused our analysis of the submergence on the period 2009 – 2018, where the impact of correction is lowest (Fig. 10).

17

420 For transferability, individual correction functions from UAV surveys must be determined for each glacier, as these are directly related to glacier-specific slope gradients, orientation, the height of the glacier tongue, and area-height distributions (Fig. 11). Additional UAV surveys, which are low-cost and more flexible, but cover smaller areas, may be conducted to determine the correction function of any glacier within the study site. This allows the adjustment of the respective DSM difference to glaciological periods and therefore a comparison with the

425 magnitudes of the glaciological data. Best results can be expected if the correction function represents the ablation processes in the period that needs corrections. If the correction function is applied to photogrammetric mass balances retrospectively, intra-annual variation must be considered. In that case, if a more detailed analysis of the annual variations is needed, a mass balance model would produce more reliable results.

Despite the above-mentioned potential causes of errors, we showed that the presented workflow to correct the

430 photogrammetric elevation changes to full multi-annual mass balances provides good results. These results agree well with the glaciological mass balances (Fig. 8), but show characteristic deviations in the elevation distribution (Fig. 9). Thus, they are (i) suitable for detecting systematic errors in the glaciological method (Fischer, 2011) and (ii) the method is transferable to other glaciers. This result is of great importance for future studies. Large-area, cadastral aerial surveys are usually recorded at any time in autumn and are therefore useless for verification of

435 glaciological measurements.

For our case, the Vernagtferner, comparing the corrected photogrammetrically derived DSM differences with interpolated rasters from glaciological measurements, revealed small-scale differences as well as general offsets due to ice dynamics (Fig. 10). Such deviations usually occur in highly crevassed areas, in debris-covered areas, due to temporal changes in the snowpack within the accumulation area, internal and basal melting and interpolation

440 errors of the glaciological method (Fischer, 2011). For crevassed areas, the deviations found at the Vernagtferner are negligible. With regard to the influence of debris cover (about 3.8 % of the total glacier surface) on the glacier mass balance, the effect results to 0.8 ± 0.6 % of the annual total mass balance, which is not represented by the spatial interpolation of the glaciological measurements at the moment. Debris-cover might play an increasing role when debris-covered glacier areas increase due to further glacier decline (Scherler et al., 2018). This could increase

445 the need to conduct high resolution geodetic observations in addition to glaciological measurements because point measurements on debris-covered parts are not always representative. Surprisingly, the differences between geodetic and glaciological volume change in the accumulation areas do not reveal large spatial deviations, even though the glaciological results rely on very sparse in situ data. This demonstrates that the long-term accumulation conditions at Vernagtferner, which are known from former detailed investigations (Mayer et al., 2013a; Mayer et

450 al., 2013b), are spatially relatively stable and can be used for scaling the point measurements. Even though this comparison of geodetic and glaciological results in the accumulation region has the potential to improve the representation of spatial variability across these areas.

Assuming that internal and basal melting are negligible, and the influence of temporal snowpack differences is small due to the long period of investigation and the rather small ratio of accumulation area, the remaining

455 differences result from the large scale dynamic processes. They become quantifiable when looking at the mean differences per altitude of both methods (Fig. 9), whereby the high spatial resolution and accuracy is absolutely crucial. It is noticeable that the switch between emergence and submergence is about 100 to 150 m below the ELA of the Vernagtferner (BADW, 2019). While the ELA increased between the two periods (2009 - 2015 vs. 2015 - 2018) by about 60 m, the change from submergence to emergence decreased by about 90 m. The reasons for this

18

460 development are unknown but might indicate a further deviation from balanced conditions during recent years. Even though the derived submergence is depending on the correction function, the values for the Vernagtferner and its accumulation areas correspond to literature values and show differences between the individual accumulation areas, which support glaciological observations. (Lambrecht et al., 2011; Mayer et al., 2013b) Future aerial image acquisitions aiming at calculating glacier mass balances must be as close as possible to each

465 other (same date within the year) and preferably at the end of the ablation season. Ideally, these acquisitions are taken close to the standard glaciological mass balance data of September 30th, to allow a direct comparison with available field information. Since aerial image surveys require cloud-free weather, it will not always be possible to acquire the images on this exact date. For this reason, temporal corrections, as successfully implemented within this study, will play an essential role in future studies. Additionally, future photogrammetric data acquisitions

470 should be as large as possible, but at least cover the entire glacier area.

7   Conclusion

This study demonstrates the high potential of aerial images and the resulting DSM's for analyzing glacier retreat in great spatial and temporal detail. For all 25 glaciers within the study area, height changes were analyzed with a 20 cm spatial resolution and compared to each other. It was shown that the glacier retreat does not only take place

475 in low altitudes, but that even high accumulation basins are meanwhile affected due to non-compensated ice flow. The altitude of the most significant glacier height changes, as well as the amount of maximum volume loss, has increased within our observation period. If all aerial surveys that are available for large parts of the Alps were used, the majority of all alpine glaciers could be analyzed by the presented method in the future. The spatial resolution of the respective analysis would be significantly higher than in other recent satellite-based studies. The

480 photogrammetric results were compared with glaciological in-situ measurements. The required correction of acquisition dates was successfully applied by using an UAV survey. This shows that the main disadvantage of using photogrammetry, not being able to survey at the right time can be reduced by using additional UAV surveys, which can be better targeted in time. This study also shows that results from the glaciological method can be greatly complemented with photogrammetric analyses, which increases the accuracy of the glaciological mass

485 balance series, reveals regions of anomalous mass balance conditions, and allows estimates of the imbalance between mass balance and ice dynamics.

The Cryosphere
Discussions

8   References

Abermann, J., Lambrecht, A., Fischer, A. and Kuhn, M.: Quantifying changes and trends in glacier area and
volume in the Austrian Ötztal Alps (1969-1997-2006), The Cryosphere, 3, 205–215,
https://doi.org/10.5194/tc-3-205-2009, 2009.

505   Auer, I., Böhm, R., Jurkovic, A., Lipa, W., Orlik, A., Potzmann, R., Schöner, W., Ungersböck, M., Matulla, C.,
Briffa, K., Jones, P., Efthymiadis, D., Brunetti, M., Nanni, T., Maugeri, M., Mercalli, L., Mestre, O.,
Moisselin, J.-M., Begert, M., Müller-Westermeier, G., Kveton, V., Bochnicek, O., Stastny, P., Lapin, M.,
Szalai, S., Szentimrey, T., Cegnar, T., Dolinar, M., Gajic-Capka, M., Zaninovic, K., Majstorovic, Z. and
Nieplova, E.: HISTALP—historical instrumental climatological surface time series of the Greater Alpine

510   Region, Int. J. Climatol., 27, 17–46, https://doi.org/10.1002/joc.1377, 2007.

Cogley, G.: Mass-balance terms revisited, Journal of Glaciology, 56, 997–1001,
https://doi.org/10.3189/002214311796406040, 2010.

Cogley, G., Hock, R., Rasmussen, L. A., Arendt, A. A. and Zemp, M.: Glossary of glacier mass balance and
related terms, 86, https://doi.org/10.5167/uzh-53475, 2011.

515   Escher-Vetter, H.: 400 Jahre Feldforschung am Vernagtferner (Ötztal, Österreich), Lozan, J. L.; Graßl, H.;
Kasang, D.; Notz, D.; Escher-Vetter, H. (5 editors) / Warnsignal Klima / Wissenschaftliche Auswertungen,
Hamburg, 299pp, ch. 4.7 (146-154), 2015.

Esri, DigitalGlobe, GeoEye, i-cubed, USDA FSA, USGS, AEX, Getmapping, Aerogrid, IGN, IGP, swisstopo
and GIS-Anwender-Community: World Imagery, 2020.

520   Fischer, A.: Comparison of direct and geodetic mass balances on a multi-annual time scale, The Cryosphere, 5,
107–124, https://doi.org/10.5194/tc-5-107-2011, 2011.

Fischer, A., Seiser, B., Stocker Waldhuber, M., Mitterer, C. and Abermann, J.: Tracing glacier changes in
Austria from the Little Ice Age to the present using a lidar-based high-resolution glacier inventory in Austria,
The Cryosphere, 9, 753–766, https://doi.org/10.5194/tc-9-753-2015, 2015a.

525   Fischer, M., Huss, M. and Hoelzle, M.: Surface elevation and mass changes of all Swiss glaciers 1980–2010,
The Cryosphere, 9, 525–540, https://doi.org/10.5194/tc-9-525-2015, 2015b.

Fliri, F.: Das Klima im Raume von Tirol, Innsbruck-München, 1975.

Fugazza, D., Scaioni, M., Corti, M., D&apos, Agata, C., Azzoni, R. Sergio, Cernuschi, M., Smiraglia, C. and
Diolaiuti, G. Adele: Combination of UAV and terrestrial photogrammetry to assess rapid glacier evolution

530   and map glacier hazards, Nat. Hazards Earth Syst. Sci., 18, 1055–1071, https://doi.org/10.5194/nhess-18-
1055-2018, 2018.

Gobiet, A., Kotlarski, S., Beniston, M., Heinrich, G., Rajczak, J. and Stoffel, M.: 21st century climate change in
the European Alps - a review, The Science of the total environment, 493, 1138–1151,
https://doi.org/10.1016/j.scitotenv.2013.07.050, 2014.

535   Hanzer, F., Förster, K., Nemec, J. and Strasser, U.: Projected cryospheric and hydrological impacts of 21st
century climate change in the Ötztal Alps (Austria) simulated using a physically based approach, Hydrology
and Earth System Sciences, 22, 1593-1614, https://doi.org/10.15488/3378, 2018.

The Cryosphere
Discussions

Open Access

EGU

Heipke, C.: Photogrammetrie und Fernerkundung, Springer, Berlin, Heidelberg, Germany, 2017.

Hirschmüller, H.: Semi-Global Matching. Motivation, Developments and Applications, available at:
540   https://elib.dlr.de/73119/1/180Hirschmueller.pdf, 2019.

Huss, M.: Extrapolating glacier mass balance to the mountain-range scale: the European Alps 1900–2100, The
        Cryosphere, 6, 713–727, https://doi.org/10.5194/tc-6-713-2012, 2012.

Huss, M.: Density assumptions for converting geodetic glacier volume change to mass change, The Cryosphere,
        7, 877–887, https://doi.org/10.5194/tc-7-877-2013, 2013.

545   Kaser, G., Fountain, A., Jansson, P., Heucke, E. and Knaus, M.: A manual for monitoring the mass balance of
        mountain glaciers, UNESCO, 137 pp., available at:
        https://globalcryospherewatch.org/bestpractices/docs/UNESCO_manual_glaciers_2003.pdf, 2003.

Lambrecht, A., Mayer, C., Hagg, W., Popovnin, V., Rezepkin, A., Lomidze, N. and Svanadze, D.: A comparison
        of glacier melt on debris-covered glaciers in the northern and southern Caucasus, The Cryosphere, 5, 525–
550   538, https://doi.org/10.5194/tc-5-525-2011, 2011.

Legat, K., Moe, K., Poli, D. and Bollmannb, E.: Exploring the potential of aerial photogrammetry for 3D
        modelling of high-alpine envirnoments, Int. Arch. Photogramm. Remote Sens. Spatial Inf. Sci., XL-3/W4,
        97–103, https://doi.org/10.5194/isprs-archives-XL-3-W4-97-2016, 2016.

Marty, C. and Meister, R.: Long-term snow and weather observations at Weissfluhjoch and its relation to other
555   high-altitude observatories in the Alps, Theor Appl Climatol, 110, 573–583, https://doi.org/10.1007/s00704-
        012-0584-3, 2012.

Mass balance of the Vernagtferner, AT: https://geo.badw.de/vernagtferner-digital/massenbilanz.html, last access:
        19 July 2019.

Mayer, C., Escher-Vetter, H. and Weber, M.: 46 Jahre glaziologische Massenbilanz des Vernagtferners,
560   Zeitschrift für Gletscherkunde und Glazialgeologie, 45/46, 219–234, 2013a.

Mayer, C., Lambrecht, A., Blumthaler, U. and Eisen, O.: Vermessung und Eisdynamik des Vernagtferners,
        Ötztaler Alpen, Zeitschrift für Gletscherkunde und Glazialgeologie, 45/46, 259–280, 2013b.

Nuth, C. and Kääb, A.: Co-registration and bias corrections of satellite elevation data sets for quantifying glacier
        thickness change, The Cryosphere, 5, 271–290, https://doi.org/10.5194/tc-5-271-2011, 2011.

565   Östrem, G.: Ice Melting under a Thin Layer of Moraine, and the Existence of Ice Cores in Moraine Ridges,
        Geografiska Annaler, 228–230, https://doi.org/10.1080/20014422.1959.11907953, 1959.

Pellikka, P. K. E. and Rees, W. G. (Eds.): Remote sensing of glaciers: techniques for topographic, spatial and
        thematic mapping of glaciers, Taylor & Francis, New York, USA, 2010.

Rogora, M., Frate, L., Carranza, M. L., Freppaz, M., Stanisci, A., Bertani, I., Bottarin, R., Brambilla, A.,
570   Canullo, R., Carbognani, M., Cerrato, C., Chelli, S., Cremonese, E., Cutini, M., Di Musciano, M.,
        Erschbamer, B., Godone, D., Iocchi, M., Isabellon, M., Magnani, A., Mazzola, L., Di Morra Cella, U., Pauli,
        H., Petey, M., Petriccione, B., Porro, F., Psenner, R., Rossetti, G., Scotti, A., Sommaruga, R., Tappeiner, U.,
        Theurillat, J.-P., Tomaselli, M., Viglietti, D., Viterbi, R., Vittoz, P., Winkler, M. and Matteucci, G.:
        Assessment of climate change effects on mountain ecosystems through a cross-site analysis in the Alps and
575   Apennines, Science of The Total Environment, 624, 1429–1442,
        https://doi.org/10.1016/j.scitotenv.2017.12.155, 2018.

Rolstad, C., Haug, T. and Denby, B.: Spatially integrated geodetic glacier mass balance and its uncertainty based on geostatistical analysis: application to the western Svartisen ice cap, Norway, J. Glaciol., 55, 666–680, https://doi.org/10.3189/002214309789470950, 2009.

580 Rossini, M., Di Mauro, B., Garzonio, R., Baccolo, G., Cavallini, G., Mattavelli, M., Amicis, M. de and Colombo, R.: Rapid melting dynamics of an alpine glacier with repeated UAV photogrammetry, Geomorphology, 304, 159–172, https://doi.org/10.1016/j.geomorph.2017.12.039, 2018.

Scherler, D., Wulf, H. and Gorelick, N.: Global Assessment of Supraglacial Debris-Cover Extents, Geophys. Res. Lett., 45, 798–805, https://doi.org/10.1029/2018GL080158, 2018.

585 Sommer, C., Malz, P., Seehaus, T. C., Lippl, S., Zemp, M. and Braun, M.: Rapid glacier retreat and downwasting throughout the European Alps in the early 21 st century, Nat Commun, 11, 1–10, https://doi.org/10.1038/s41467-020-16818-0, 2020.

Zekollari, H., Huss, M. and Farinotti, D.: Modelling the future evolution of glaciers in the European Alps under the EURO-CORDEX RCM ensemble, The Cryosphere, 13, 1125–1146, https://doi.org/10.5194/tc-13-1125-
590   2019, 2019.

Zemp, M., Thibert, E., Huss, M., Stumm, D., Rolstad Denby, C., Nuth, C., Nussbaumer, S. U., Moholdt, G., Mercer, A., Mayer, C., Joerg, P. C., Jansson, P., Hynek, B., Fischer, A., Escher-Vetter, H., Elvehøy, H. and Andreassen, L. M.: Reanalysing glacier mass balance measurement series, The Cryosphere, 7, 1227–1245, https://doi.org/10.5194/tc-7-1227-2013, 2013.

595